

Supplementary Information (ESI)

Manuscript ID AY-ART-03-2014-000542

Gold nanoparticles for design of smart colorimetric logic gates operations and scavengers for mercury ions in water

Anshu Kumar , Parimal Paul

S. No.	Title	Page No.
1	Fig. S1 (A) the absorbance ratio A_{649}/A_{520} of DM-AuNPs with $H_2PO_4^-$ (20 μM) with different concentrations of AuNPs at pH 7.0. (B) The absorbance ratio A_{649}/A_{520} of DM-AuNPs (1.9 nM) $H_2PO_4^-$ (20 μM) at different pH.	S3
2	Fig. S2 Plot of the absorbance ratio A_{649}/A_{520} for DM-AuNPs (1.9 nM) with increasing concentration of $H_2PO_4^-$.	S4
3	Fig. S3 UV-vis spectral changes for the citrate stabilized AuNPs with incremental addition of DM (0, 0.06, 0.08, 0.1, 0.2, 0.4, 0.6, 0.8, 1, 2, 4, 6, 9, 10, 11, 12 and 20 μM) in the presence of 20 μM $H_2PO_4^-$. Inset: plot of A_{649}/A_{520} vs concentration of DM, only linear portion ($R^2 = 0.991$) is shown.	S5
4	Fig. S4(a) Plot of absorption ratios A_{649}/A_{520} corresponding to the concentration of DM in the range 0.06-20 μM in presence of 20 μM $H_2PO_4^-$ and (b) Photographic image of AuNPs with incremental addition of DM in the concentration range 0.06 - 20 μM .	S6
5	Fig. S5 The plot of the ratio of A_{649}/A_{520} vs time from the UV-vis spectral change obtained from the solution containing 1.9 nM AuNPs and (a) 20 μM $H_2PO_4^-$ +10 μM DM , (b) 10 μM DM and (c) 40 μM $H_2PO_4^-$ and its respective TEM images.	S7
6	Fig. S6 A nonimplication logic gate system consisting AuNPs by using 20 μM $H_2PO_4^-$ (1) and 4 μM DM (2) analytes as inputs. (a) Illustration of the operational design of the AND gate. (b) Truth table of the AND gate. (c) Equivalent electronic circuit for the nonimplication logic operation.	S8
7	Fig. S7 Results of nonimplication logic gate with different input	S9

	modes were characterized by colorimetric and UV–vis detection (a), the corresponding logic readout in the form of A_{649}/A_{520} (b), TEM images (c) and photographic image (d).	
8	Fig. S8 Absorption spectra of DM, $H_2PO_4^-$ and both in the absence and presence of Hg^{2+} .	S10
9	Fig. S9 ESI MS spectrum of the $[DM-Hg^{2+}]$ complex.	S11
10	Fig. S10 TEM images of the AuNPs-Hg system. (A, B, and C) of different regions (1.9 nm AuNPs) after treated with 4 μM Hg^{2+} and its EDX data.	S12
11	Fig. S11 The UV-vis spectra of the cit-AuNPs (red), after treatment with DM and $H_2PO_4^-$ (aggregated-AuNPs), purple), and aggregated-AuNPs treated with Hg^{2+} (reddish brown).	S13
12	Fig. S12 A Plot of absorption ratios A_{649}/A_{520} of aggregated-AuNPs corresponding to the concentration of Hg^{2+} in the range 0.002-20 μM .	S14
13	Fig. S13 A Plot of absorption ratios A_{649}/A_{520} of aggregated-AuNPs corresponding to the concentration of Hg^{2+} in the range 0.002-0.8 μM .	S15
14	Fig. S14 Removal of Hg^{2+} from the lake water. Microscope image of the precipitate taken at 40X magnification and zoom.	S16

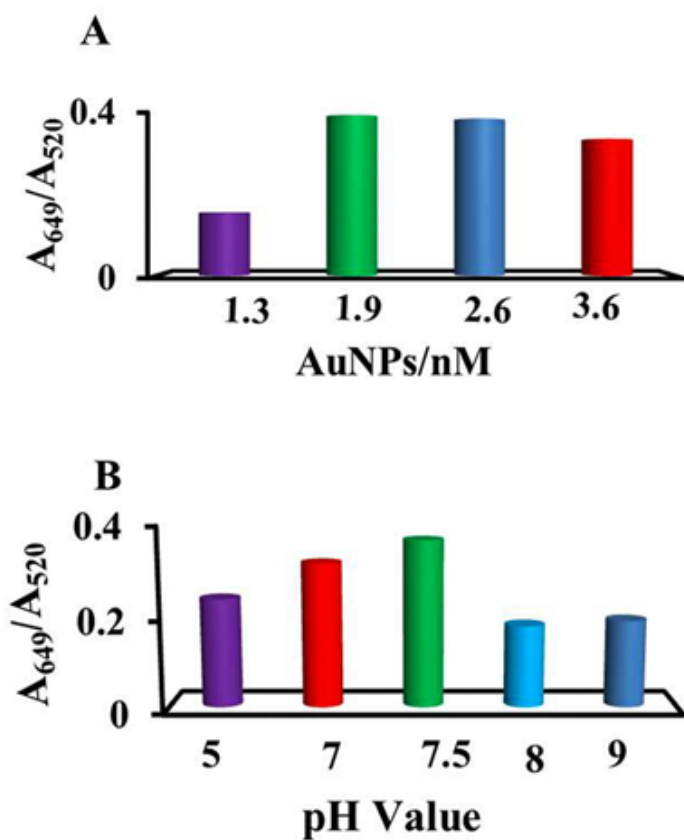


Fig. S1 (A) the absorbance ratio A_{649}/A_{520} of DM-AuNPs with $H_2PO_4^-$ (20 μM) with different concentrations of AuNPs at pH 7.0. (B) The absorbance ratio A_{649}/A_{520} of DM-AuNPs (1.9 nM) $H_2PO_4^-$ (20 μM) at different pH.

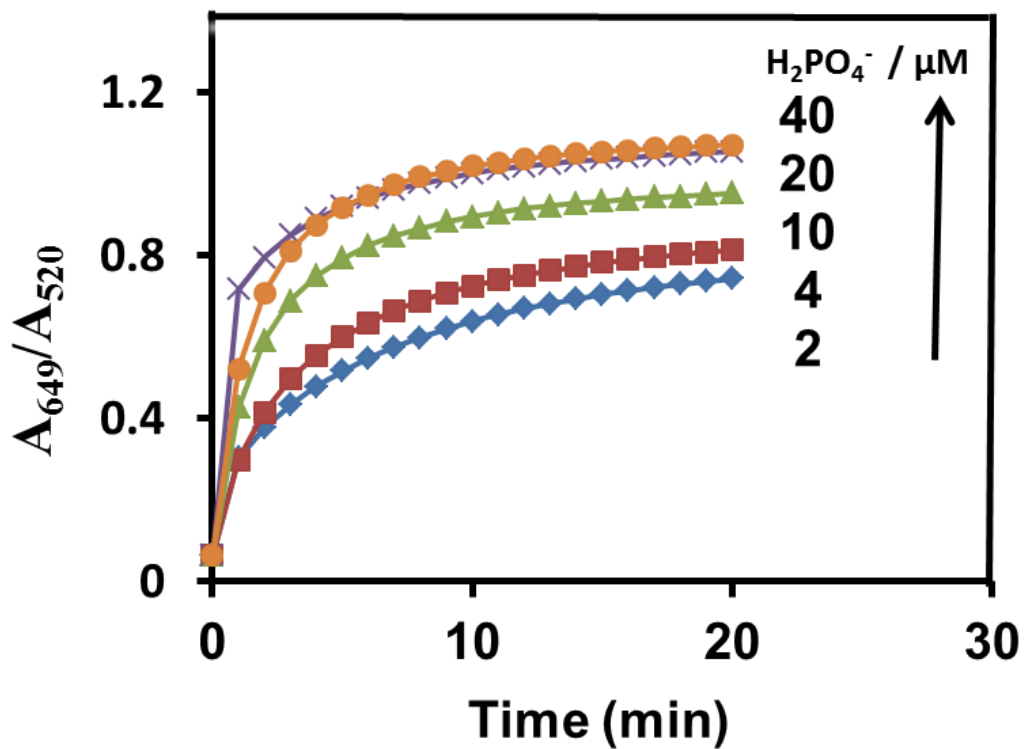


Fig. S2 Plot of the absorbance ratio A_{649}/A_{520} for DM-AuNPs (1.9 nM) with increasing concentration of $H_2PO_4^-$

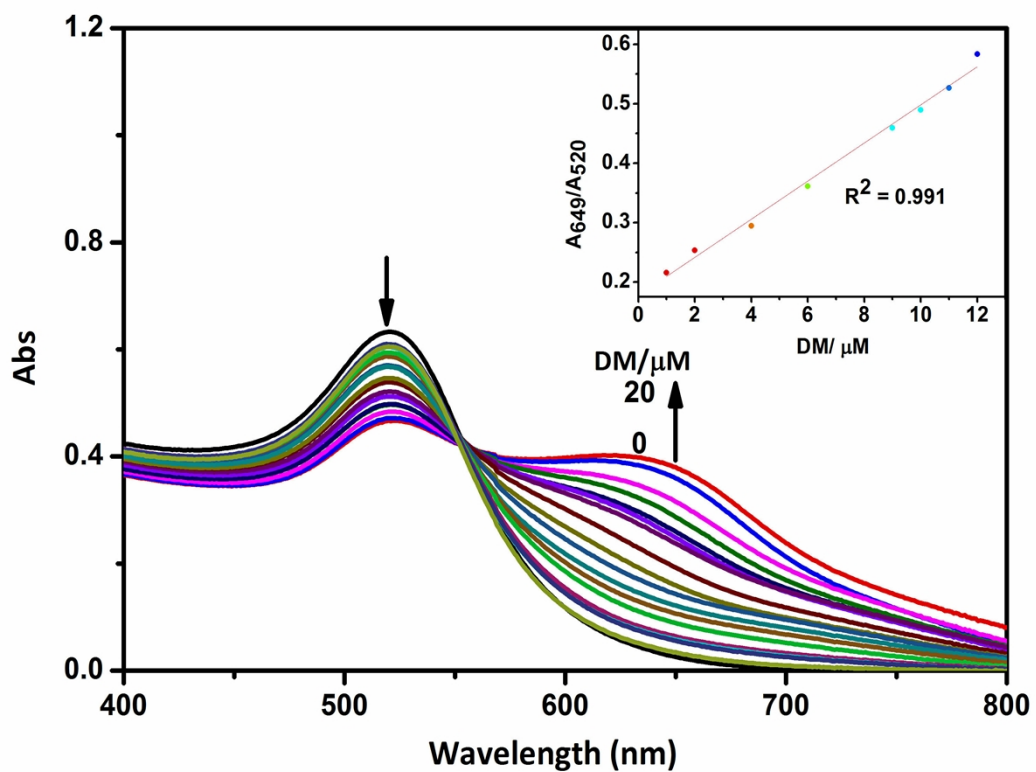


Fig. S3 UV-vis spectral changes for the citrate stabilized AuNPs with incremental addition of DM (0, 0.06, 0.08, 0.1, 0.2, 0.4, 0.6, 0.8, 1, 2, 4, 6, 9, 10, 11, 12 and 20 μM) in the presence of 20 μM H_2PO_4^- . Inset: plot of A_{649}/A_{520} vs concentration of DM, only linear portion ($R^2 = 0.991$) is shown.

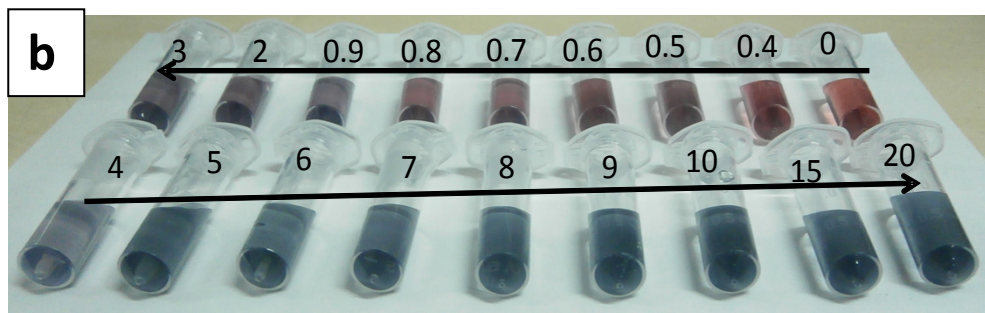
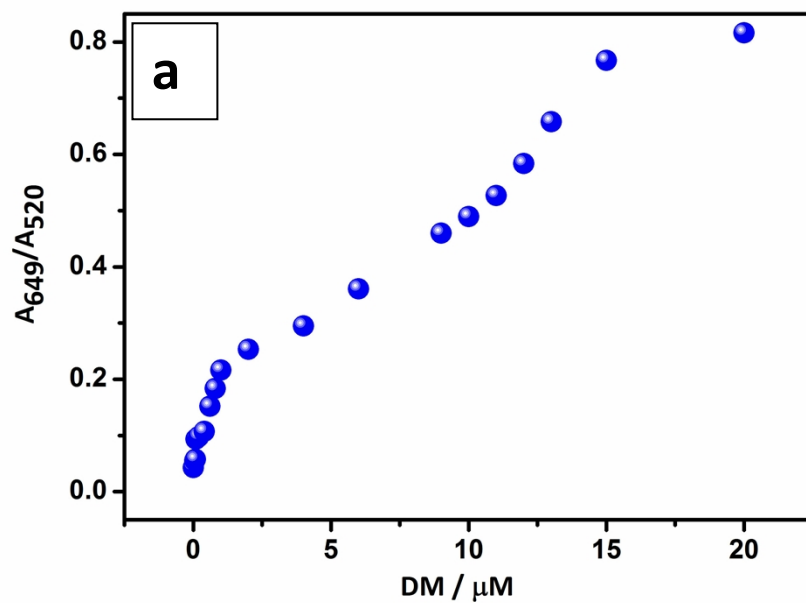


Fig. S4(a) Plot of absorption ratios A_{649}/A_{520} corresponding to the concentration of DM in the range 0.06-20 μM in presence of 20 μM H_2PO_4^- and **(b)** Photographic image of AuNPs with incremental addition of DM in the concentration range 0.06 - 20 μM .

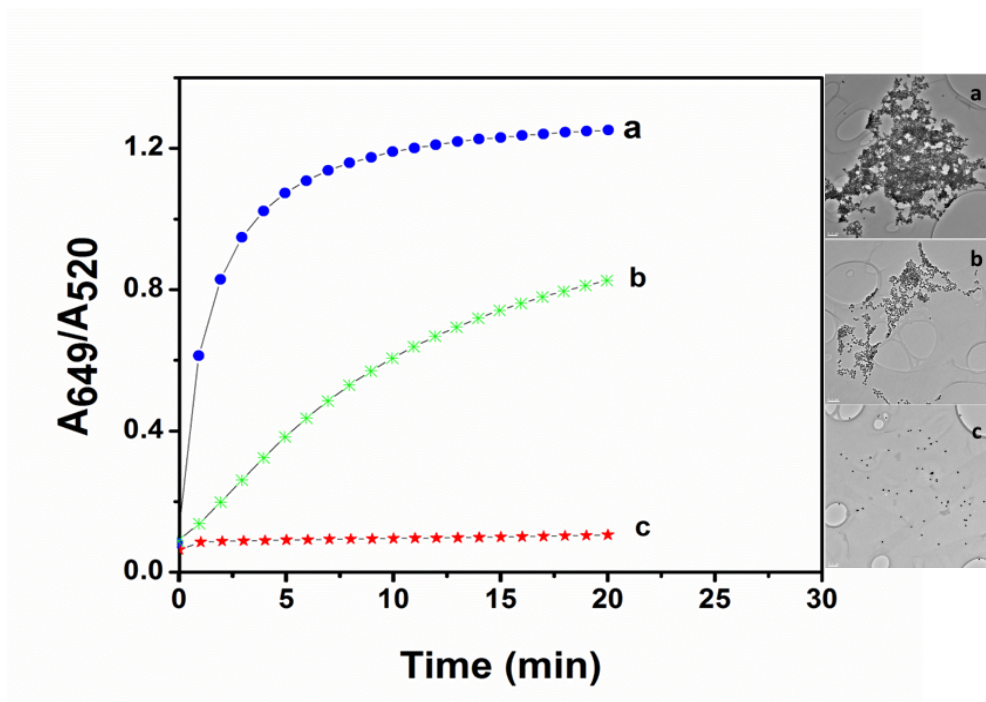


Fig. S5 The plot of the ratio of A_{649}/A_{520} vs time from the UV-vis spectral change obtained from the solution containing 1.9 nM AuNPs and (a) 20 μM H_2PO_4^- +10 μM DM , (b) 10 μM DM and (c) 40 μM H_2PO_4^- and its respective TEM images.

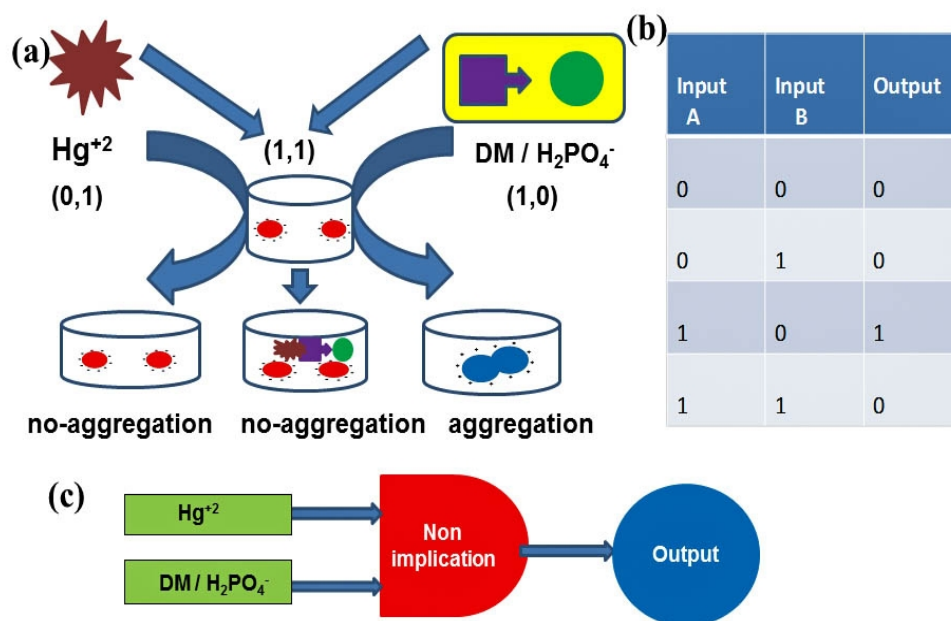


Fig. S6 A nonimplication logic gate system consisting AuNPs by using 20 μM H_2PO_4^- (1) and 4 μM DM (2) analytes as inputs. (a) Illustration of the operational design of the AND gate. (b) Truth table of the AND gate. (c) Equivalent electronic circuit for the nonimplication logic operation.

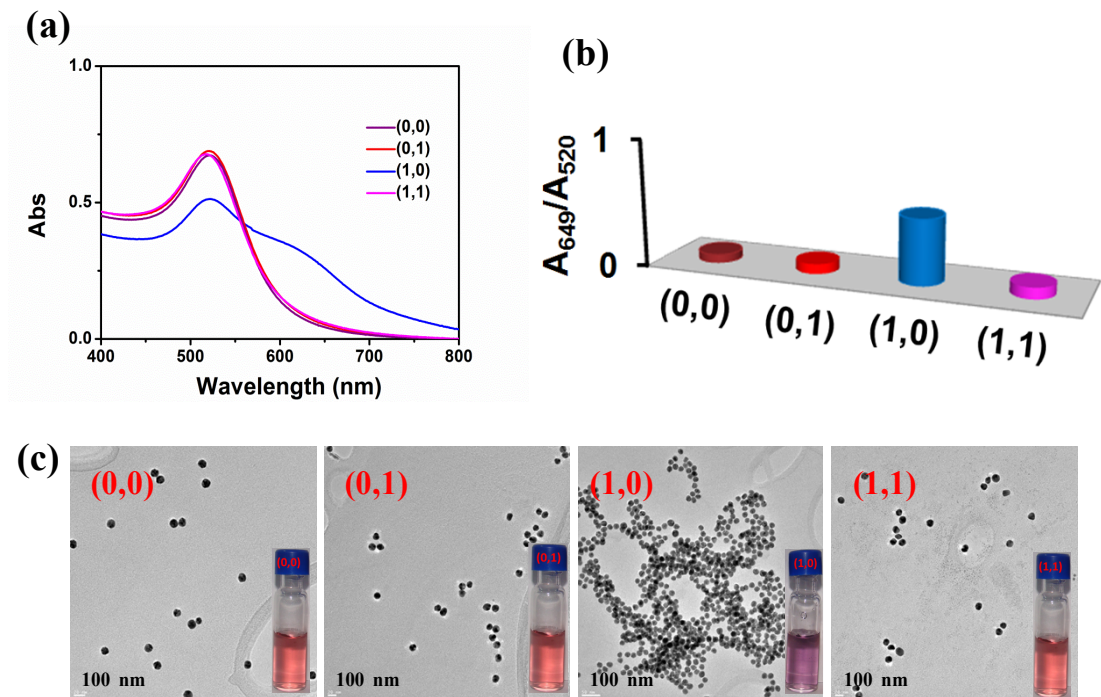


Fig. S7 Results of nonimplication logic gate with different input modes were characterized by colorimetric and UV-vis detection (a), the corresponding logic readout in the form of A_{649}/A_{520} (b), TEM images (c) and photographic image (d).

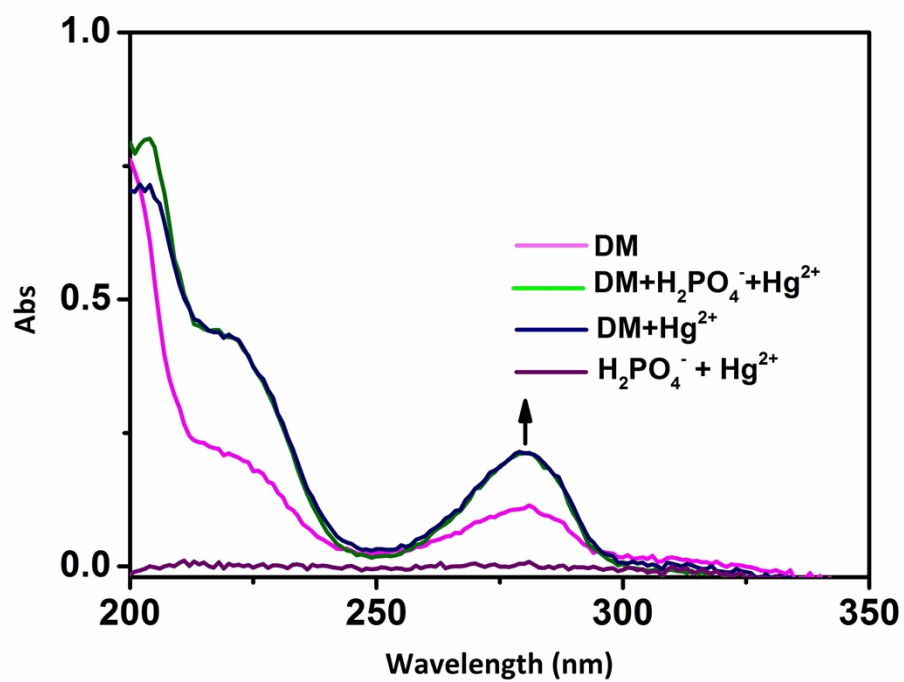


Fig. S8 Absorption spectra of DM, H₂PO₄⁻ and both in the absence and presence of Hg²⁺

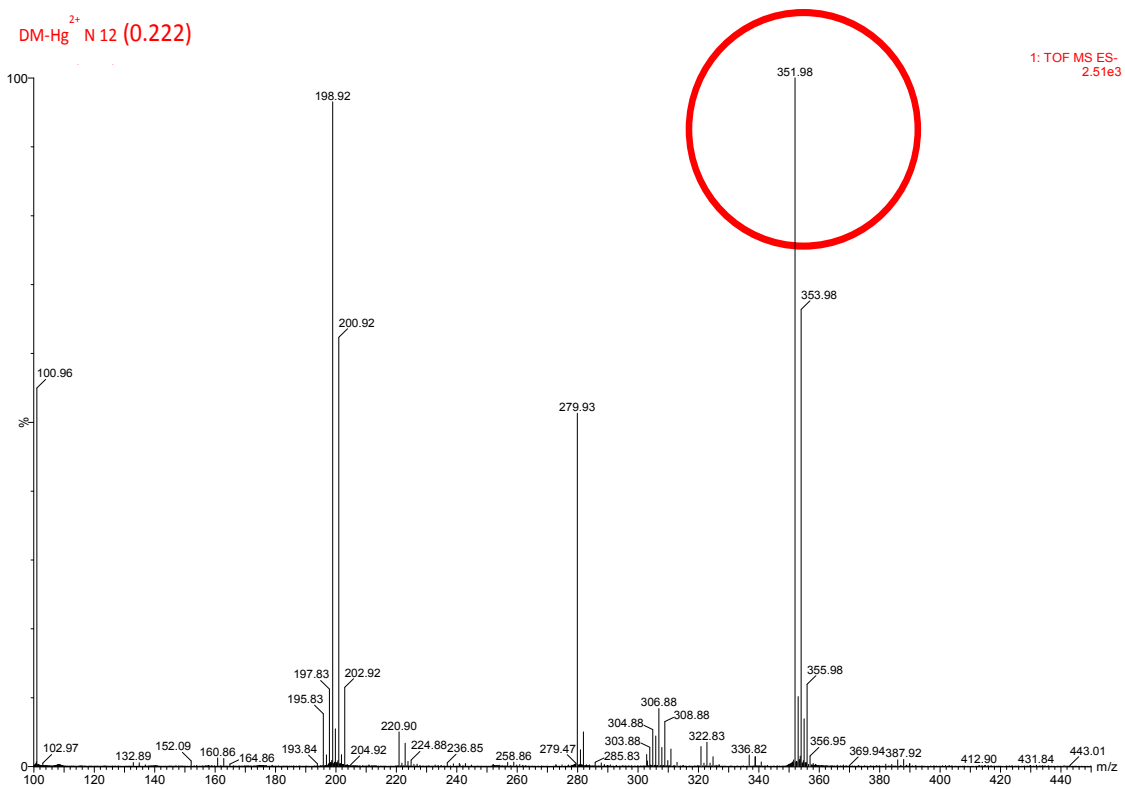


Fig. S9 ESI MS spectrum of the [DM-Hg²⁺] complex.

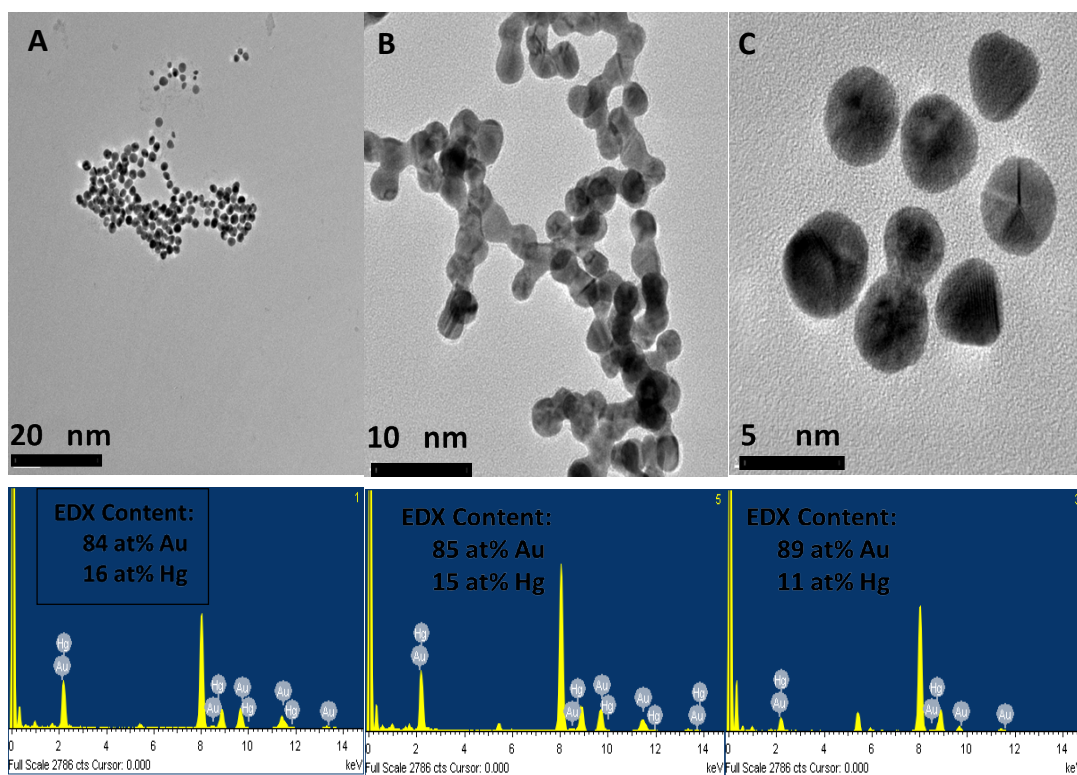


Fig. S10 TEM images of the AuNPs-Hg system. (A, B and C) of different regions (1.9 nM AuNPs) after treated with 4 μM Hg^{2+} and its EDX data.

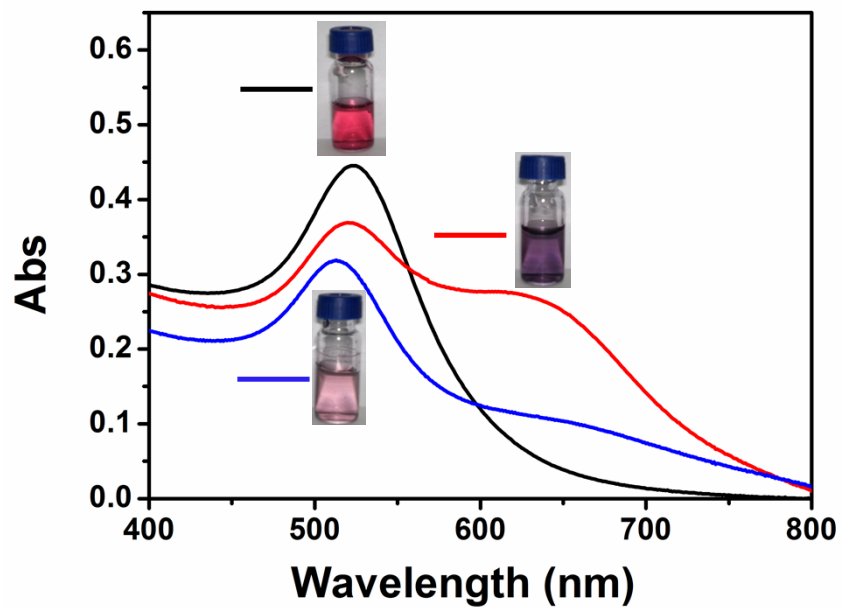


Fig. S11 The UV-vis spectra of the cit-AuNPs (red), after treatment with DM and H_2PO_4^- (aggregated-AuNPs), purple), and aggregated-AuNPs treated with Hg^{2+} (reddish brown).

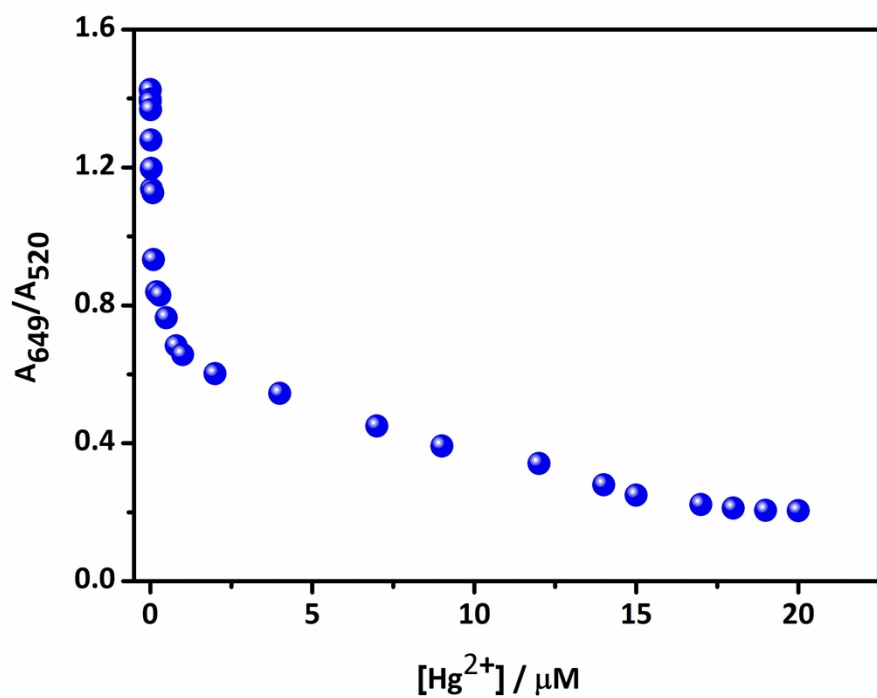


Fig. S12 A Plot of absorption ratios A_{649}/A_{520} of aggregated-AuNPs corresponding to the concentration of Hg^{2+} in the range 0.002-20 μM .

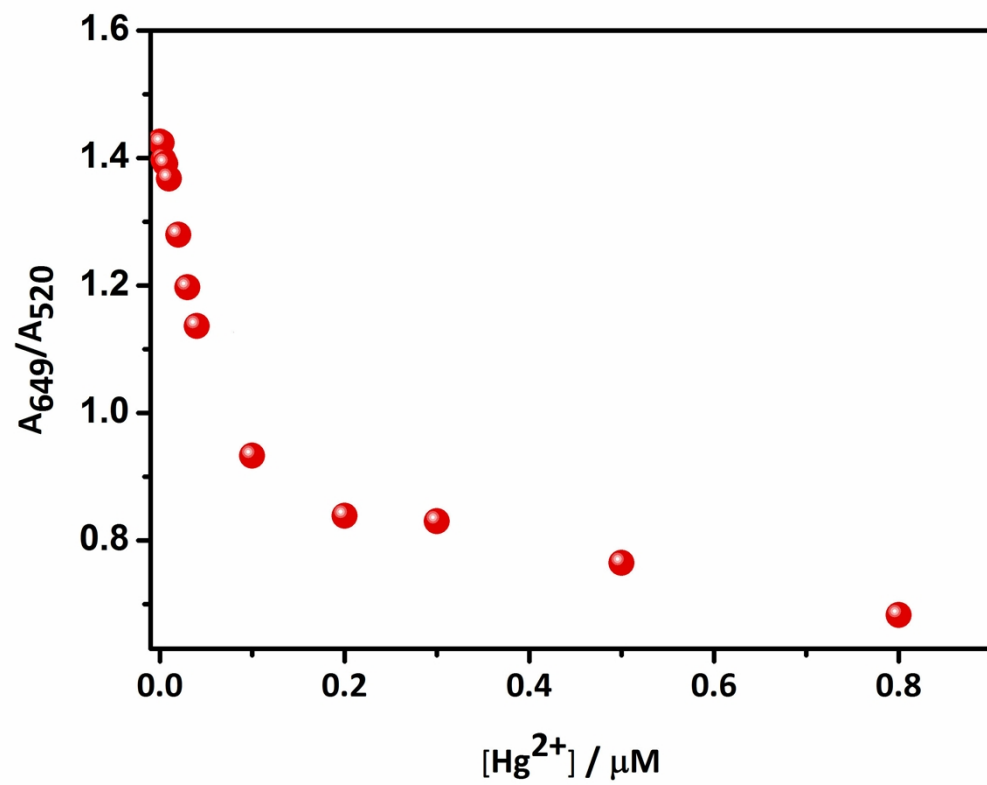


Fig. S13 A Plot of absorption ratios A_{649}/A_{520} of aggregated-AuNPs corresponding to the concentration of Hg^{2+} in the range 0.002-0.8 μM .

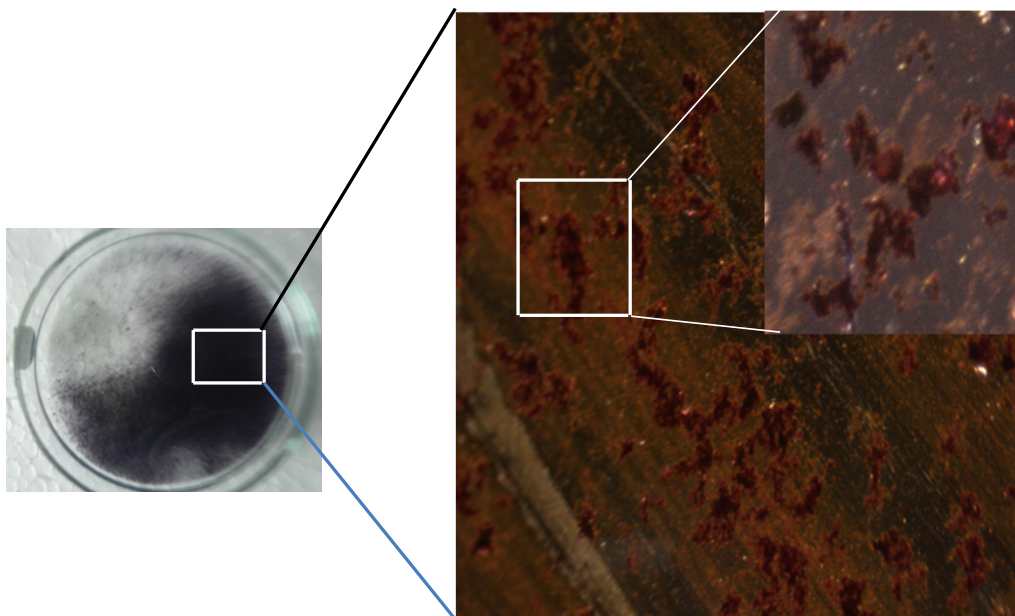


Fig. S14 Removal of Hg^{2+} from the lake water. Microscope image of the precipitate taken at 40X magnification and zoom